

1 **New Asymptotic and Pre-Asymptotic Results on Rainfall Maxima from Multifractal**  
2 **Theory**

3  
4  
5 By

6 Daniele Veneziano<sup>1</sup>, Andreas Langousis<sup>1</sup> and Chiara Lepore<sup>2</sup>

7  
8 (1) Department of Civil and Environmental Engineering, MIT, Cambridge, MA,  
9 02139, USA

10  
11 (2) Parsons Laboratory for Environmental Science and Engineering, MIT,  
12 Cambridge, MA 02139, USA

13  
14  
15  
16  
17 Submitted to  
18 *Water Resources Research*

19  
20  
21 Submitted: May, 2009

22  
23 Revised: August, 2009

24  
25  
26  
27  
28  
29  
30  
31  
32  
33 -----  
34 \*Corresponding author: Andreas Langousis, Dept. of Civil and Environmental Engineering, MIT, Room 1-245,  
35 Cambridge, MA, 02139. Tel: 617-407-0059, andlag@gmail.com.

## Abstract

36  
37  
38  
39  
40  
41  
42  
43  
44  
45  
46  
47  
48  
49  
50  
51  
52  
53  
54  
55  
56  
57  
58

Contrary to common belief, Fisher-Tippett's extreme value (EV) theory does not typically apply to annual rainfall maxima. Similarly, Pickands' extreme excess (EE) theory does not typically apply to rainfall excesses above thresholds on the order of the annual maximum. This is true not just for long averaging durations  $d$ , but also for short  $d$  and in the high-resolution limit as  $d \rightarrow 0$ . We reach these conclusions by applying large deviation theory to multiplicative rainfall models with scale-invariant structure. We derive several asymptotic results. One is that, as  $d \rightarrow 0$ , the annual maximum rainfall intensity in  $d$ ,  $I_{yr,d}$ , has generalized extreme value (GEV) distribution with a shape parameter  $k$  that is significantly higher than that predicted by EV theory and is always in the EV2 range. The value of  $k$  does not depend on the upper tail of the marginal distribution, but on regions closer to the body. Under the same conditions, the excesses above levels close to the annual maximum have generalized Pareto distribution with parameter  $k$  that is always higher than that predicted by Pickands' EE theory. For finite  $d$ , the distribution of  $I_{yr,d}$  is not GEV, but in accordance with empirical evidence is well approximated by a GEV distribution with shape parameter  $k$  that increases as  $d$  decreases. We propose a way to estimate  $k$  under pre-asymptotic conditions from the scaling properties of rainfall and suggest a near-universal  $k(d)$  relationship. The new estimator promises to be more accurate and robust than conventional estimators. These developments represent a significant conceptual change in the way rainfall extremes are viewed and evaluated.

**Keywords:** rainfall maxima, extreme value theory, extreme excess theory, large deviations, IDF curves

59

## 1. Introduction

60 This paper deals with the classical problem of characterizing the distribution of annual rainfall  
 61 maxima. Let  $I_d$  be the average rainfall intensity in an interval of duration  $d$  and  $I_{yr,d}$  be the  
 62 maximum of  $I_d$  in one year. A long-standing tenet of stochastic hydrology is that, at least for  $d$   
 63 small, the distribution of  $I_{yr,d}$  is of the generalized extreme value (GEV) type; see e.g. Chow *et*  
 64 *al.* (1988), Singh (1992), and Stedinger *et al.* (1993). This belief stems from the fact that, if  
 65 under suitable normalization the maximum of  $n$  independent and identically distributed (*iid*)  
 66 variables is attracted as  $n \rightarrow \infty$  to a non-degenerate distribution  $G_{\max}$ , then  $G_{\max}$  must have the  
 67 GEV form

$$68 \quad G_{\max}(x) = \exp \left\{ - \left[ 1 + k \left( \frac{x - \psi}{\lambda} \right) \right]^{-1/k} \right\} \quad (1)$$

69 where  $\lambda$ ,  $\psi$  and  $k$  are scale, location and shape parameters, respectively. Methods to estimate  
 70 extreme rainfall intensities from recorded annual maxima (e.g. Koutsoyiannis *et al.*, 1998;  
 71 Martins and Stedinger, 2000; Gellens, 2002; Overeem *et al.*, 2008) are generally based on this  
 72 result.

73 The specific form of the distribution (EV1 when the shape parameter  $k = 0$ , EV2 when  $k >$   
 74  $0$  and EV3 when  $k < 0$ ) depends on the upper tail of the parent distribution, in our case the  
 75 distribution of  $I_d$  (Gumbel, 1958). For  $k = 0$ , equation (1) reduces to the Gumbel (EV1) form  
 76  $F(x) = \exp \{ -\exp(-(x - \psi)/\lambda) \}$  with an exponential extreme upper tail, whereas for positive  $k$   
 77 the distribution is Frechet (EV2) whose upper tail behaves like a power function with exponent  
 78  $-1/k$ . Thus, for the same probability of exceedance, larger values of  $k$  are associated with higher

79 rainfall intensities and more extreme behavior of the rainfall process. For negative  $k$  the  
80 distribution is Weibull (EV3), with a finite upper bound.

81 Another pillar of extreme rainfall modelling is extreme excess (EE) theory. Let  $X$  be a  
82 random variable with distribution  $F$ . The excess of  $X$  above  $u$ ,  $X_u = (X - u | X \geq u)$ , has  
83 distribution  $F_u(x) = \frac{F(u+x) - F(u)}{1 - F(u)}$ . Pickands (1975) derived limiting properties of  $F_u$  that  
84 parallel the results of extreme value theory for the maxima. He found that, as  $u$  increases and  
85  $F(u) \rightarrow 1$ : (1) the distribution of  $X_u$  converges to a non-degenerate distribution  $G_{exc}$  if and only  
86 if the maximum of  $n$  *iid* copies of  $X$  converges to a non-degenerate distribution  $G_{max}$ ; (2)  $G_{exc}$   
87 has generalized Pareto (GP) form; and (3)  $G_{exc}$  has the same shape parameter  $k$  as  $G_{max}$  in  
88 equation (1).

89 An important property of the GP distribution is that the maximum of a Poisson number of  
90 *iid* GP( $k$ ) variables has GEV( $k$ ) distribution with the same  $k$  (e.g. Stedinger *et al.*, 1993). In  
91 conjunction with Pickands' results, this property has been extensively used in Peak-over-  
92 Threshold (PoT) and Partial-Duration-Series (PDS) methods of extreme rainfall analysis. Peak-  
93 over-Threshold methods generally assume that the peak of  $I_d$  above some high threshold  $u$  has  
94 GP distribution and find the (GEV) distribution of the annual maximum assuming that  $I_d$  up-  
95 crosses level  $u$  at Poisson times; see e.g. Smith (1985), Leadbetter (1991) and, Madsen *et al.*  
96 (1997). Partial-Duration-Series methods do the same using the marginal excesses of  $I_d$  above  $u$ ;  
97 see e.g. Stedinger *et al.* (1993), Beirlant *et al.* (1996) and Martins and Stedinger (2001a,b).

98 We question whether the distribution of the annual maximum  $I_{yr,d}$  is in fact GEV and has  
99 the shape parameter  $k$  of  $G_{max}$  in equation (1). This is clearly not the case for long durations  $d$ ,  
100 say  $d > 1$  week, because  $n = (1 \text{ year})/d$  is too small. However, extreme value (EV) theory might

101 become relevant to  $I_{yr,d}$  as  $d \rightarrow 0$ , since then  $n \rightarrow \infty$ . Similarly, we question whether as  $d \rightarrow 0$   
102 the excesses of  $I_d$  above thresholds on the order of the annual maximum have GP distribution  
103 with the same  $k$  as  $G_{\max}$ . We address these issues by using stationary models of rainfall in  
104 which rainfall intensity at different scales satisfies a scale invariance condition. These  
105 (multifractal) models have been found to accurately predict rainfall extremes (Veneziano *et al.*,  
106 2006a; Langousis and Veneziano, 2007).

107 We find that, under stationarity and multifractality, EV theory does not apply to the annual  
108 maximum, because for any given  $d$  the block size  $n$  needed for reasonable convergence to the  
109 asymptotic GEV distribution far exceeds (1 year)/ $d$ . We are especially interested in the annual  
110 maxima at small scales, for which an appropriate framework is provided by large deviation (LD)  
111 theory (on LD theory, see e.g. Dembo and Zeitouni, 1993 and Den Hollander, 2000). Using LD  
112 tools, we obtain several new asymptotic results. One is that, as  $d \rightarrow 0$ , the annual maximum  
113  $I_{yr,d}$  approaches an EV2 distribution with a shape parameter  $k$  that is always higher than that  
114 predicted by extreme value theory. Interestingly,  $k$  does not depend on the upper tail of  $I_d$  but on  
115 regions of the distribution closer to the body and can be obtained in a simple way from the  
116 scaling properties of the rainfall process. Similarly, as  $d \rightarrow 0$ , the excess of  $I_d$  above thresholds  
117 on the order of  $I_{yr,d}$  has  $GP(k)$  distribution, where  $k$  is the same as for  $I_{yr,d}$  and therefore is  
118 always higher than the value from Pickands' theory.

119 We also study the distribution of  $I_{yr,d}$  under pre-asymptotic conditions ( $d$  finite). These are  
120 the conditions of greatest interest in practice. In this case the distribution of  $I_{yr,d}$  is not GEV and  
121 in fact may differ significantly from any EV or LD asymptotic distribution, but over a finite  
122 range of quantiles is accurately approximated by a GEV distribution with parameter  $k$  that  
123 decreases as  $d$  increases. This dependence of  $k$  on  $d$  is in accordance with much empirical

124 evidence; see e.g. Asquith (1998), Mohyont *et al.* (2004), Trefry *et al.* (2005), Veneziano *et al.*  
125 (2007) and Section 4 below. We propose a method to estimate  $k(d)$  from the scaling properties of  
126 the rainfall process and the range of quantiles (or return periods) of interest. The multifractal  
127 parameters provide a linkage between  $k$  and the local precipitation climate. We also suggest a  
128 near-universal default  $k(d)$  relationship for use at non-instrumented sites.

129 Section 2 describes the rainfall model (a simple sequence of discrete multifractal cascades)  
130 and recalls results on the upper tail of  $I_d$  for such cascades from LD theory. Section 3 derives  
131 asymptotic properties of the  $N$ -year maximum  $I_{Nyr,d}$  in the small-scale limit  $d \rightarrow 0$  for cases  
132 with  $N$  fixed and  $N$  that varies as a power law of the averaging duration  $d$ . Section 3 derives also  
133 corresponding properties of the excess of  $I_d$  above thresholds on the order of  $I_{Nyr,d}$ . Section 4  
134 focuses on the distribution of the annual maximum under pre-asymptotic conditions and Section  
135 5 summarizes the main conclusions and outlines future steps.

136 In subsequent sections we make a change of notation, as follows. An important parameter  
137 of stationary multifractal processes is the upper limit  $D$  of the durations  $d$  for which the process  
138 displays scale invariance (e.g. Schertzer and Lovejoy, 1987; Gupta and Waymire, 1990;  
139 Veneziano, 1999; Langousis *et al.*, 2007). In the analysis of such processes, what matters is not  
140 the duration  $d$  but the resolution  $r = D/d$  relative to  $D$ . Accordingly, we use  $I_r, I_{yr,r}$  and  $I_{Nyr,r}$  in  
141 place of  $I_d, I_{yr,d}$  and  $I_{Nyr,d}$ , respectively. Since the analysis is confined to the scaling range, we  
142 only consider resolutions  $r \geq 1$ .

## 143 **2. Multiplicative and Multifractal Rainfall Models**

144 There is ample evidence that the fluctuations of rainfall intensity at different scales combine in a  
145 multiplicative way; see e.g. Over and Gupta (1996), Perica and Foufoula-Georgiou (1996),

146 Veneziano *et al.* (1996), Venugopal *et al.* (1999), Deidda (2000), and Veneziano and Langousis  
 147 (2005a). Multiplicative models represent rainfall intensity  $I(t)$  as

$$148 \quad I(t) = m \prod_{j=1}^{\infty} Y_j(t) \quad (2)$$

149 where  $m$  is the mean rainfall intensity and the processes  $Y_j(t)$  are non-negative, independent,  
 150 with mean value 1. These processes contribute fluctuations at characteristic temporal scales  $d_j$   
 151 or equivalently at resolutions  $r_j = D/d_j > 1$  relative to some large reference scale  $D$ . Since for  
 152 our analysis the mean value does not matter, in what follows we set  $m = 1$ .

153 In the case of multifractal models, the resolutions  $r_j$  satisfy  $r_j = b^j$  for some  $b > 1$  and  
 154  $Y_1(t), Y_2(t), \dots$  are contractive transformations of the same stationary random process  $Y(t)$ ,  
 155 meaning that  $Y_j(t)$  is equivalent to  $Y(r_j t)$ ; see e.g. Veneziano (1999). An important special case  
 156 is when  $Y(t)$  is a process with constant *iid* values inside consecutive  $D$  intervals and  $b$  is an  
 157 integer  $\geq 2$ . Then equation (2) generates a sequence of *iid* discrete multifractal cascades of  
 158 multiplicity  $b$  within consecutive  $D$  intervals (on discrete multifractal cascades, see e.g. Schertzer  
 159 and Lovejoy, 1987; Gupta and Waymire, 1990; and Evertsz and Mandelbrot, 1992). Discrete-  
 160 cascade sequences of this type have been found to reproduce well the intensity-duration-  
 161 frequency (IDF) curves extracted from historical records or generated by more sophisticated  
 162 rainfall models (Langousis and Veneziano, 2007).

163 In a discrete-cascade representation of rainfall, the average rainfall intensity in a generic  
 164 cascade tile at resolution  $r_j$ ,  $I_{r_j}$ , satisfies

$$165 \quad \begin{aligned} I_{r_j} &= A_{r_j} Z \\ A_{r_j} &= Y_1 Y_2 \cdots Y_j, \end{aligned} \quad j = 0, 1, \dots \quad (3)$$

166 where  $A_{r_0} = 1$ , the factors  $Y_1, \dots, Y_j$  are independent copies of a non-negative variable  $Y$  with  
 167 mean value 1, and  $Z$  is a mean-1 “dressing factor.” Each  $Y_i$ ,  $i \leq j$ , models the effect on  $I_{r_j}$  of the  
 168 rainfall intensity fluctuations at resolution  $r_i$ , while  $Z$  captures the combined effect of all  
 169 multiplicative fluctuations at resolutions higher than  $r_j$ ; see Kahane and Peyriere (1976) and  
 170 Schertzer and Lovejoy (1987).

171 An important feature of the distribution of  $Z$  is the asymptotic Pareto upper tail (i.e.  $P[Z > z]$   
 172  $\sim z^{-q^*}$ ) where  $q^* > 1$  is the order at or beyond which the moments of  $Z$  diverge. The distribution  
 173 of  $Z$  does not have analytical form, but it can be calculated numerically using the procedure of  
 174 Veneziano and Furcolo (2003), or approximated analytically; see Langousis *et al.* (2007).

175 To realistically represent rainfall, one must model both the alternation of dry and wet  
 176 conditions and the fluctuations of rainfall intensity during the rainy periods. This requires  $Y$  to  
 177 have a non-zero probability mass at zero. A frequent choice is  $Y = Y_\beta Y_{LN}$ , where  $Y_\beta$  is a discrete  
 178 random variable with probability mass  $P_0$  at zero and probability mass  $1 - P_0$  at  $1/(1 - P_0)$  and  $Y_{LN}$   
 179 is a lognormal variable with mean value 1 (e.g. Over and Gupta, 1996; Langousis *et al.*, 2007).  
 180 In the multifractal literature, processes with  $Y = Y_\beta$  are called “beta” processes, while those with  
 181  $Y = Y_{LN}$  are referred to as “lognormal” processes, although the marginal distribution is not  
 182 exactly lognormal due to the dressing factor  $Z$ ; see equation (3). When  $Y = Y_\beta Y_{LN}$ , we say that  
 183 the process is “beta-lognormal” (beta-LN) and refer to the distribution of  $Y$  as a beta-LN  
 184 distribution. The scaling properties of a beta-LN process depend on the probability  $P_0$  and the  
 185 variance of  $\ln(Y_{LN})$  (see below for an alternative parameterization).

186 Later sections make frequent use of the moment-scaling function

$$187 \quad K(q) = \log_{r_j} (E[A_{r_j}^q]) = \log_b (E[Y^q]) \quad (4)$$

188 and its Legendre transform  $C(\gamma)$  given by

$$189 \quad C(\gamma) = \max_q \{\gamma q - K(q)\}, \quad K(q) = \max_\gamma \{\gamma q - C(\gamma)\} \quad (5)$$

190 In the beta-LN case, these functions are

$$191 \quad \begin{aligned} K(q) &= C_\beta(q-1) + C_{LN}(q^2 - q), & q \geq 0 \\ C(\gamma) &= \frac{C_{LN}}{4} \left( \frac{\gamma - C_\beta}{C_{LN}} + 1 \right)^2 + C_\beta, & \gamma \geq \gamma_{\min} \end{aligned} \quad (6)$$

192 where  $C_\beta = -\log_b(1 - P_0)$  and  $C_{LN} = 0.5 \text{Var}[\log_b(Y_{LN})]$  provide an alternative parameterization  
 193 of the distribution of  $Y$  and  $\gamma_{\min} = C_\beta - C_{LN}$  is the slope of  $K(q)$  at 0. For example, in fitting a  
 194 beta-LN model to a rainfall record from Florence, Italy, Langousis and Veneziano (2007) found  
 195  $D \approx 15$  days,  $C_\beta \approx 0.4$  and  $C_{LN} \approx 0.05$ . Figure 1 shows qualitative plots of the  $K(q)$  and  $C(\gamma)$   
 196 functions and indicates quantities of interest for the analysis that follows. Although for the  
 197 present analysis the values of  $C_\beta$  and  $C_{LN}$  and more in general the distribution of  $Y$  do not  
 198 matter, we use these settings to exemplify the theoretical results.

199 In the next section we need to evaluate how, in the small-scale limit  $j \rightarrow \infty$ , exceedance  
 200 probabilities of the type  $P[I_{r_j} > r_j^\gamma]$  depend on the resolution  $r_j$  and the exponent  $\gamma$ . For this we  
 201 turn to large deviation (LD) theory (e.g. Dembo and Zeitouni, 1993). Specifically, Cramer's  
 202 Theorem (Cramer, 1938) gives an asymptotic expression for the probability with which the sum  
 203 of  $j$  *iid* variables exceeds levels proportional to  $j$ , as  $j \rightarrow \infty$ . One might think that as  $j \rightarrow \infty$  the  
 204 sum should have a normal distribution, but as  $j$  increases the quantiles of interest move into more  
 205 extreme tail regions where the sum has not yet converged to the normal distribution. If for the  
 206 moment one neglects the dressing factor  $Z$  in equation (3), then  $I_{r_j} = A_{r_j}$  and Cramer's Theorem

207 is directly relevant to our problem because  $P[A_{r_j} > r_j^\gamma] = P[\sum_{i=1}^j \log_b(Y_i) > \gamma]$ . One can extend  
 208 Cramer's results to include the dressing factor  $Z$ ; see Veneziano (2002). This extension gives

$$209 \quad P[A_{r_j} Z > r_j^\gamma] \sim \begin{cases} r_j^{-C(\gamma)}, & \gamma_{\min} \leq \gamma \leq \gamma^* \\ r_j^{-C(\gamma^*) - q^*(\gamma - \gamma^*)}, & \gamma > \gamma^* \end{cases} \quad (7)$$

210 where  $\sim$  denotes equality up to a factor  $g(r_j, \gamma)$  that varies slowly (slower than a power law) with  
 211  $r_j$  at infinity,  $C(\gamma)$  and  $K(q)$  are the functions in equation (5),  $q^* > 1$  is the moment order such  
 212 that  $K(q^*) = q^* - 1$ , and  $\gamma^*$  is the slope of  $K(q)$  at  $q^*$ . For  $C(\gamma)$  and  $K(q)$  in equation (8),  
 213  $q^* = (1 - C_\beta) / C_{LN}$  and  $\gamma^* = 2 - C_\beta - C_{LN}$ . The asymptotic behavior of  $g(r_j, \gamma)$  as  $j \rightarrow \infty$  is  
 214 known (Veneziano, 2002), but for the present objectives it is sufficient to work with the “rough  
 215 limits” in equation (7).

216 The result in equation (7) for  $\gamma < \gamma^*$  is also the limiting behavior of  $P[A_{r_j} > r_j^\gamma]$  produced  
 217 by Cramer's Theorem. The reason is that, for  $\gamma_{\min} \leq \gamma \leq \gamma^*$  and  $j$  large, the dressing factor  $Z$   
 218 contributes a factor to the probability  $P[A_{r_j} Z > r_j^\gamma]$  that does not depend on  $j$  and therefore can  
 219 be absorbed into the function  $g(r_j, \gamma)$ . By contrast, for  $\gamma > \gamma^*$  and  $j$  large, the probability  
 220  $P[A_{r_j} Z > r_j^\gamma]$  is dominated by the Pareto tail of  $I_{r_j}$ , which has the form  $P[I_{r_j} > i] \propto i^{-q^*}$  and  
 221 starts at  $i^* \sim r_j^{\gamma^*}$  (Langousis *et al.*, 2007). This power-law tail originates from the Pareto tail of  
 222 the dressing factor  $Z$ ; see comments following equation (3).

### 223 3. Asymptotic Analysis

224 In practice, one is interested in the distribution of the annual maximum  $I_{yr,r}$  for finite  
 225 resolutions  $r$  and the distribution of the excess  $I_{r,u}$  for finite  $r$  and thresholds  $u$  on the order of

226  $I_{yr,r}$ . Before studying these pre-asymptotic properties (see Section 4), we examine the behaviour  
 227 of the  $N$ -year maximum  $I_{Nyr,r}$  and the excess  $I_{r,u}$  for thresholds  $u$  on the order of  $I_{Nyr,r}$  under  
 228 various asymptotic conditions. This asymptotic analysis produces extensions of extreme value  
 229 (EV) and extreme excess (EE) results and clarifies why those theories do not apply to the annual  
 230 rainfall maxima. We consider two cases: the classical limit ( $r$  fixed,  $N \rightarrow \infty$ ) and the non-  
 231 classical limit ( $r \rightarrow \infty$ ,  $N = cr^\alpha$ ) for any given  $c > 0$  and  $\alpha$ . When  $\alpha = 0$ , the latter limit becomes  
 232 ( $r \rightarrow \infty$ ,  $N = c$  fixed) and thus characterizes the distribution of the  $c$ -year maximum of  $I_r$  at  
 233 small scales. To simplify notation, we denote the resolution by  $r$ , with the understanding that in a  
 234 discrete cascade model  $r$  is constrained to have values  $r_j = b^j$ . An important property of  
 235 multifractal cascades that we use below is that, for resolutions  $r$  larger than about 2 and return  
 236 periods  $T$  of practical interest (say  $T/D \approx 10^2 - 10^6$ ), the distribution of  $I_{Nyr,r}$  is accurately  
 237 approximated by the distribution of the maximum of  $rN/D$  independent copies of  $I_r$ , where  $D$  is  
 238 in years; see Langousis *et al.* (2007).

239 Consider first the limiting case ( $r$  finite,  $N \rightarrow \infty$ ). As we have noted at the end of Section 2,  
 240 the dressing factor  $Z$  causes  $I_r$  to have an algebraic upper tail of the type  $P[I_r > i] \propto i^{-q^*}$ , with  
 241  $q^*$  in equation (7). It follows from classical extreme value theory that, as  $N \rightarrow \infty$ ,  $I_{Nyr,r}$  is  
 242 attracted to EV2( $1/q^*$ ), an EV2 distribution with shape parameter  $k^* = 1/q^*$ . It also follows that  
 243 the excess above thresholds on the order of the  $N$ -year maximum is attracted to GP( $1/q^*$ ), a  
 244 generalized Pareto distribution with the same shape parameter  $k^*$ .

245 The case ( $r \rightarrow \infty$ ,  $N = cr^\alpha$ ) is more interesting and produces new results. Our first step is  
 246 to investigate the asymptotic behavior of the distribution of  $I_r$  for intensities in the range of the  
 247  $cr^\alpha$ -year maximum. By this we mean the range between the  $\varepsilon$ - and  $(1-\varepsilon)$ -quantiles of  $I_{cr^\alpha yr,r}$ ,

248 where  $\varepsilon$  is a positive number arbitrarily close to 0. We denote these quantiles by  $i_{\max,\varepsilon}$  and  
 249  $i_{\max,1-\varepsilon}$ , respectively. To examine the distribution of  $I_r$  within this range in the small-scale  
 250 limit, we need the exceedance probabilities  $P[I_r > i_{\max,\varepsilon}]$  and  $P[I_r > i_{\max,1-\varepsilon}]$  as  $r \rightarrow \infty$ . Under  
 251 the assumption that rainfall intensities in non-overlapping  $(D/r)$ -intervals are independent (as  
 252 indicated above, this assumption produces accurate approximations of the maximum  
 253 distribution), these probabilities are given by

$$254 \quad \begin{aligned} P_\varepsilon &= P[I_r > i_{\max,\varepsilon}] = 1 - \varepsilon^{1/n} \\ P_{1-\varepsilon} &= P[I_r > i_{\max,1-\varepsilon}] = 1 - (1 - \varepsilon)^{1/n} \end{aligned} \quad (8)$$

255 where  $n = cr^{1+\alpha}/D$ , with  $D$  expressed in years, is the number of  $(D/r)$ -intervals in  $cr^\alpha$  years.  
 256 Considering that  $\varepsilon$  is very small,  $P_{1-\varepsilon} \approx \varepsilon/n$ . One can further show that, for any given  $\varepsilon$ ,  
 257  $P_\varepsilon = 1 - \varepsilon^{1/n} \rightarrow \frac{\ln(1/\varepsilon)}{n}$  as  $n \rightarrow \infty$ . Therefore, for any given  $\varepsilon > 0$ , as  $(r \rightarrow \infty, N = cr^\alpha)$  the range  
 258  $[i_{\max,\varepsilon}, i_{\max,1-\varepsilon}]$  corresponds to intensities  $i$  with exceedance probabilities  
 259  $P[I_r > i] = \eta/n = \eta D/(cr^{1+\alpha})$ , where  $\varepsilon < \eta < \ln(1/\varepsilon)$  is positive and finite.

260 Appendix A uses equation (7) and the above results to show that, in the  $(r \rightarrow \infty, N = cr^\alpha)$   
 261 limit and for  $\varepsilon < \eta < \ln(1/\varepsilon)$ , the intensity  $i$  that is exceeded by  $I_r$  with probability  
 262  $\eta D/(cr^{1+\alpha})$  varies with  $r$ ,  $\eta$  and  $\alpha$  as

$$263 \quad i \sim \begin{cases} r^{\gamma_{1+\alpha}} \eta^{-1/q_{1+\alpha}}, & \alpha_{\min} < \alpha < \alpha^* \\ r^{\gamma^* + (\alpha - \alpha^*)/q^*} \eta^{-1/q^*}, & \alpha \geq \alpha^* \end{cases} \quad (9)$$

264 where  $\gamma_{1+\alpha}$  satisfies  $C(\gamma_{1+\alpha}) = 1 + \alpha$ ,  $q_{1+\alpha}$  is such that the slope  $K'(q_{1+\alpha}) = \gamma_{1+\alpha}$ ,  $q^*$  and  $\gamma^*$  are  
 265 the same as in equation (7),  $\gamma^* = K'(q^*)$ ,  $\alpha^* = C(\gamma^*) - 1 = q^*(\gamma^* - 1)$ , and  $\alpha_{\min} = -K(0) - 1$ .

266 Some of these quantities are illustrated in Figure 1. Note that the results in equation (9) do not  
 267 depend on the outer scale of multifractal behavior  $D$  or the constant  $c$ .

268 What is important for our analysis is that  $i$  in equation (9) varies with  $\eta$  like  $\eta^{-k_\alpha}$  with

$$269 \quad k_\alpha = \begin{cases} 1/q_{1+\alpha}, & \alpha_{\min} < \alpha < \alpha^* \\ 1/q^*, & \alpha \geq \alpha^* \end{cases} \quad (10)$$

270 From this power-law behavior of  $I_r$  in the range of the  $cr^\alpha$ -year maximum we conclude that the  
 271 maximum itself must be attracted to an EV2( $k_\alpha$ ) distribution with  $k_\alpha$  in equation (10). It also  
 272 follows that, in the range of thresholds and intensities that satisfy  $[i_{\max,\varepsilon} < u, I_{r,u} + u < i_{\max,1-\varepsilon}]$ ,  
 273 the excess  $I_{r,u}$  is attracted to a GP( $k_\alpha$ ) distribution (generalized Pareto, with the same shape  
 274 parameter  $k_\alpha$ ). Note that  $k^* = 1/q^*$ , the value of  $k_\alpha$  for  $\alpha \geq \alpha^*$ , coincides with the shape  
 275 parameter of the asymptotic GEV distribution from EV/EE theory.

276 For example, in the case of beta-LN processes, the parameters in equation (9) are

$$277 \quad \begin{aligned} \gamma_{1+\alpha} &= C_\beta - C_{LN} + 2\sqrt{C_{LN}(1+\alpha-C_\beta)}, & q_{1+\alpha} &= \sqrt{(1+\alpha-C_\beta)/C_{LN}} \\ \gamma^* &= 2 - C_\beta - C_{LN}, & q^* &= (1-C_\beta)/C_{LN} \\ \alpha_{\min} &= C_\beta - 1, & \alpha^* &= (1-C_\beta)(q^* - 1) \end{aligned} \quad (11)$$

278 and the shape parameter  $k_\alpha$  in equation (10) is  
 279

$$280 \quad k_\alpha = \begin{cases} \sqrt{C_{LN}/(1+\alpha-C_\beta)}, & C_\beta - 1 < \alpha < \alpha^* \\ C_{LN}/(1-C_\beta), & \alpha \geq \alpha^* \end{cases} \quad (12)$$

281 The value  $\alpha = 0$  is of special interest, as in this case the maximum is over a constant number of  
 282 years  $N$  (including  $N = 1$  for the annual rainfall maxima). For  $\alpha = 0$ , equation (12) gives  
 283  $k_0 = \sqrt{C_{LN}/(1-C_\beta)} = \sqrt{k^*}$ , where  $k^*$  is the value of  $k$  for  $\alpha \geq \alpha^*$  (as well as the value of  $k$   
 284 from EV theory).

285 Figure 2 shows how  $k_\alpha$  in equation (12) varies with  $\alpha$  for beta-LN processes. The  
286 expressions in the figure are generic for any scaling parameters  $C_\beta$  and  $C_{LN}$ , but the plot is for  
287  $C_\beta = 0.4$  and  $C_{LN} = 0.05$ , which are realistic values for rainfall. As one can see, for all  $\alpha < \alpha^*$   
288 the parameter  $k_\alpha$  exceeds the value  $k^*$  from EV theory and diverges as  $\alpha \rightarrow \alpha_{\min} = C_\beta - 1$ . For  
289  $\alpha = 0$ , the constraint  $C_\beta + C_{LN} < 1$  implies  $k_0 < 1$ . For the specific values of  $C_\beta$  and  $C_{LN}$  used  
290 in the figure,  $k^* = 0.083$  and  $k_0 = 0.289$ . Hence EV theory severely under-predicts the shape  
291 parameter  $k$  of the annual maximum in the small-scale limit. This under-prediction results in  
292 unconservative intensity-duration-frequency (IDF) values for long return periods.

293 The main conceptual results of this section are illustrated in Figure 3. The coordinate axes  
294 are the resolution  $r = D/d$  and the number of independent  $I_r$  variables over which the maximum  
295 is taken. For the  $N$ -year maximum, this number is  $n(r) = Nr/D$ , where  $D$  is in years. The scale is  
296 logarithmic in both variables. Extreme value (EV) analysis gives that, for any given  $r$ , as  $N \rightarrow \infty$   
297 the distribution of the maximum converges to an EV2( $k^*$ ), where  $k^* = 1/q^*$ . The frequent use of  
298 this result for the annual maximum ( $N = 1$ ) is based on the implicit assumption that a relatively  
299 low block size  $n_0$  (see dashed horizontal line in Figure 3) is sufficient for convergence of the  
300 maximum to EV2( $k^*$ ). If this is not true for low  $r$  because  $n(r) = r/D$  is too small, the  
301 distribution of the maximum should be EV2( $k^*$ ) at higher resolutions for which  $r/D \gg n_0$ .  
302 Figure 3 shows that (a) when  $r$  is relatively small, reasonable convergence of the maximum to  
303 EV2( $k^*$ ) requires block sizes  $n(r)$  that are  $10^3 - 10^4$  times the annual block size  $r/D$ ; hence,  
304 unless  $N \approx (10^3 - 10^4)$  years, the  $N$ -year maximum cannot be assumed to have EV2( $k^*$ )  
305 distribution, and (b) the threshold  $n_0$  is not constant, but increases with increasing  $r$  as  $n_0 \sim$   
306  $r^{1+\alpha^*}$ , with  $\alpha^* \approx 7$ ; the latter value of  $\alpha$  is obtained from equation (12), using realistic values of

307  $C_\beta$  and  $C_{LN}$  from Figure 6.b; see Section 4 below. Since  $1 + \alpha^* \gg 1$ , as  $r$  increases the  
 308 threshold on  $n(r)$  above which EV theory applies moves farther away from the available block  
 309 size  $r/D$ . This makes the EV results even less relevant at high resolutions. Based on these results,  
 310 we conclude that, under multifractality, EV theory (and for the same reasons EE theory) does not  
 311 apply to annual rainfall extremes.

312 For a number of years  $N = cr^\alpha$ , the block size is  $n(r) = cr^{1+\alpha}/D$ , where  $D$  is in years.  
 313 Therefore, as  $r$  increases, one moves in Figure 3 along straight lines with slope  $(1 + \alpha)$ . For  
 314  $\alpha > \alpha^*$ , one eventually enters the region where EV theory holds and, as  $r \rightarrow \infty$ , the maximum  
 315 becomes EV2( $k^*$ ); see equation (10). It follows from the same equation that, for  $\alpha < \alpha^*$  and as  
 316  $r \rightarrow \infty$ , the  $cr^\alpha$ -year maximum is attracted to an EV2( $k_\alpha$ ) distribution with  $k_\alpha$  in equation (12).

317 Summarizing, in the context of multifractal models, large deviation (LD) theory extends  
 318 the results on rainfall extremes beyond the classical context of extreme value (EV) and extreme  
 319 excess (EE) theories. Specifically, the latter theories deal with the maximum of  $I_r$  at fixed  
 320 resolution  $r$  over an infinitely long period of time, whereas LD theory produces results for  
 321  $r \rightarrow \infty$  and periods of time that are either constant or diverge as power laws of  $r$ .

#### 322 **4. Pre-Asymptotic Distribution of the Annual Maximum and GEV Approximations**

323 In practice, one is interested in the annual maximum rainfall  $I_{yr,r}$  over a finite range of  
 324 resolutions. The associated points  $(r, r/D)$  in Figure 3 are typically far from the regions where the  
 325 EV, EE and LD theories apply. For these  $(r, r/D)$ -combinations the distribution of  $I_{yr,r}$  is not  
 326 GEV, but over a finite range of exceedance probabilities  $P$  or equivalently of return periods  $T =$   
 327  $1/P$ , it may be accurately approximated by a GEV distribution. Indeed, one often finds that  
 328 GEV( $k$ ) distributions fit well annual maximum data, with  $k$  being an increasing function of  $r$ . If

329 one could relate the best-fitting  $k$  to the resolution  $r$  and the multifractal parameters  $C_\beta$  and  
330  $C_{LN}$ , then one could develop a new estimator of  $k$  based on scaling theory: i.e. based on the  
331 estimates of the multifractal parameters  $C_\beta$  and  $C_{LN}$  from empirical records. This would be a  
332 valuable finding, since  $k$  is notoriously difficult to infer directly from annual maxima; see e.g.  
333 Mohymont *et al.* (2004) and Koutsoyiannis (2004). Moreover, linking  $k(r)$  to  $C_\beta$  and  $C_{LN}$   
334 would shed light on what rainfall-climate factors control the shape of the annual maximum  
335 distribution.

336 First we investigate whether, over a range of return periods  $T$ , the theoretical distribution of  
337  $I_{yr,r}$  from the multifractal model in Section 2 is approximately GEV. For this purpose, we  
338 calculate the exact distribution of  $I_{yr,r}$  for various  $(C_\beta, C_{LN})$ -combinations and different  
339 resolutions  $r$  using the method of Langousis *et al.* (2007) assuming independence of rainfall in  
340 different  $D$  intervals within a year. Then we plot this exact distribution on GEV( $k$ ) paper, varying  
341  $k$  until the resulting plot in a given range of  $T$  is closest to a straight line in a least-squares sense.  
342 As an example, the top row of Figure 4 shows these best linear fits for a beta-lognormal cascade  
343 with parameters ( $C_\beta = 0.4$ ,  $C_{LN} = 0.05$ ,  $D = 15$  days) and gives the associated values of  $k$  for  $r$   
344 = 1 and 512 in the return-period range  $2 < T < 10\,000$  years. For comparison, the lower rows in  
345 Figure 4 show similar plots on GEV( $k$ ) paper for  $k = 0$  (EV1 distribution),  $k^* = 1/q^* = 0.083$   
346 (EV2 distribution predicted by EV and EE theories), and  $k_0 = 1/q_1 = 0.289$  (EV2 distribution  
347 from LD theory under  $r \rightarrow \infty$ ). It is clear that when  $k$  is optimized (top row), GEV( $k$ )  
348 distributions provide accurate approximations to the exact distribution, whereas fixing  $k$  to 0,  
349  $1/q^*$  or  $1/q_1$  generally produces poor fits. We have repeated the analysis using different ranges of  
350 return periods, a denser set of resolutions  $r$  and different multifractal parameters. In all cases the  
351 quality of the best fit is comparable to that in the top row of Figure 4. As one may expect from

352 the top-row panels of Figure 4, the least-squares  $k$  is insensitive to the range of return periods  
353 used in the least-squares fit. For example,  $k$  is almost the same when best fitting a  $GEV(k)$   
354 distribution in the ranges from 2 to 100, 2 to 1000, or 2 to 10 000 years.

355 For the same multifractal process as in Figure 4, Figure 5.a shows plots of the best-fitting  $k$   
356 (in the  $2 < T < 100$  years range) against  $r$ . The vertical bars are  $(m \pm \sigma)$  intervals for the  
357 probability weighted moments (PWM) estimator of  $k$  applied to 60 series of 100 annual  
358 maximum values, each extracted from a 100-year continuous multifractal process simulation; on  
359 the PWM method of parameter estimation, see e.g. Hosking (1990, 1992), Koutsoyiannis (2004)  
360 and Trefry *et al.* (2005). For reference, the values  $k^* = 1/q^*$  and  $k_0 = 1/q_1$  are shown as dashed  
361 horizontal lines. As  $r \rightarrow \infty$ ,  $k$  approaches  $1/q_1$ , but over the range of resolutions considered,  $k$   
362 remains far from this limit. The mean of the estimator follows closely the least-squares  $k$  line,  
363 except for a slight negative bias at low resolutions. As one can see, even with 100 years of data  
364 the PWM estimator has high variability. Figure 5.b compares the least-squares  $k$  from Figure 5.a  
365 with values of  $k$  from the literature. These values were obtained from annual maximum rainfall  
366 records of different lengths using the probability weighted moment (PWM) method. The  
367 empirical values have a wide scatter, which is broadly consistent with the sampling variability in  
368 Figure 5.a. The theoretical best-fitting  $k$  values (for  $C_\beta = 0.4$ ,  $C_{LN} = 0.05$  and  $D = 15$  days) are  
369 generally higher, but have a dependence on  $r$  similar to the empirical values. Larger values of  $k$   
370 correspond to a thicker upper tail and, hence, higher upper quantiles of the annual maximum  
371 distribution. Possible reasons for the theoretical values being higher are negative bias of the  
372 empirical estimators and deviations of actual rainfall from the multifractal model used to produce  
373 the theoretical estimates. The latter include variations in the multifractal parameters ( $C_\beta$ ,  $C_{LN}$ ,  
374  $D$ ) and deviations from strict scale invariance; see e.g. Menabde *et al.* (1997), Schmitt *et al.*

375 (1998), Olsson (1998), Güntner *et al.* (2001), Veneziano *et al.* (2006b) and Veneziano and  
 376 Langousis (2009). These sources of discrepancy will be the subject of future investigations. It is  
 377 remarkable (but possibly coincidental) that the only empirical results based on a very extensive  
 378 data set [169 daily records, each having 100-154 years of data (Koutsoyiannis, 2004); see “K”  
 379 point in Figure 5.b] are almost identical to the theoretical values.

380 Figure 6.a compares the variation of the least-squares  $k$  value with  $r$  for selected  
 381 combinations of  $C_\beta$  and  $C_{LN}$ . Generally,  $k$  increases as either parameter increases. However, if  
 382 one considers the relative small spatial variation of these parameters (see Figure 6.b where  $C_\beta$   
 383 and  $C_{LN}$  estimates from different rainfall records are plotted against the local mean annual  
 384 precipitation  $\bar{I}_{yr}$ ), the sensitivity of  $k$  in Figure 6.a is modest. As Figure 6.b shows,  $C_{LN}$  may be  
 385 considered constant around 0.053, whereas  $C_\beta$  has a linear decreasing trend with  $\bar{I}_{yr}$ . The  
 386 default  $k$  curve in Figure 6.c has been obtained by using the  $(C_\beta, C_{LN})$  combinations in Figure  
 387 6.b and ensemble averaging the results. The dashed lines in the same figure are bounds  
 388 considering the variability of  $C_\beta$  in Figure 6.b. If one uses higher values of  $C_\beta$  in more arid  
 389 climates, as suggested by Figure 6.b,  $k$  would be slightly higher.

390 The solid line in Figure 6.c is close to the following analytical expression:

$$391 \quad k = 2.44 [\log_{10}(r) + 0.557]^{0.035} - 2.362 \quad (13)$$

392 whereas the dashed lines deviate by approximately  $\pm 0.03$ - $0.05$  (depending on the resolution  
 393  $r = D/d$ ) from the default  $k$  values in equation (13).

## 394 **5. Conclusions**

395 A long tradition links the modeling and analysis of rainfall extremes to Fisher-Tippett’s extreme-  
 396 value (EV) and Pickands’ extreme-excess (EE) theories. This includes methods that use annual-

397 maximum and peak-over-threshold rainfall information. However, for realistic rainfall models,  
398 neither theory applies. The basic reason is that the annual maxima depend on a range of the  
399 marginal distribution much below its upper tail. This realization has profound consequences on  
400 the distribution of the annual maxima and on methods for its estimation.

401 To prove these points and obtain new results on rainfall extremes, we have used stationary  
402 rainfall models with multifractal scale invariance below some temporal scale  $D$ . This scale may  
403 be seen as the time between consecutive synoptic systems capable of generating rainfall; see  
404 Langousis and Veneziano (2007). Stationary multifractal models are non-negative random  
405 processes in which the fluctuations at different scales combine in a multiplicative way and for  
406 equal log-scale increments have statistically identical amplitude. These models have received  
407 significant attention in the precipitation literature, including rainfall extremes. For multifractal  
408 models, one can use a branch of asymptotic probability theory known as large deviations (LD) to  
409 extend the limiting results from EV and EE theories. Specifically we have found that, as the  
410 averaging duration  $d \rightarrow 0$  or equivalently the resolution  $r = D/d \rightarrow \infty$ , the distribution of the  
411 annual maximum  $I_{yr,r}$  is GEV with shape parameter  $k$  in the EV2 range. Under the same  
412 asymptotic conditions, the excess of the marginal rainfall intensity  $I_r$  above thresholds  $u$  on the  
413 order of the annual maximum  $I_{yr,r}$  has generalized Pareto (GP) distribution with the same shape  
414 parameter  $k$ . The value of  $k$  is much higher than that produced by EV and EE theories and can be  
415 found theoretically from the scaling properties of the rainfall process. These asymptotic results  
416 hold also for the distribution of the  $N$ -year maximum  $I_{Nyr,r}$  for any finite  $N$  and the excesses of  
417  $I_r$  above thresholds on the order of  $I_{Nyr,r}$ .

418 With added generality, LD theory gives the asymptotic distribution of  $I_{cr^\alpha yr,r}$ , the  $(cr^\alpha)$ -  
419 year maximum, for any  $c > 0$  and  $\alpha \geq \alpha_{\min}$  where  $\alpha_{\min} < 0$  is a certain lower bound. As  $r \rightarrow \infty$ ,

420 the distribution of  $I_{cr^\alpha yr, r}$  is again EV2, with shape parameter  $k_\alpha$  that: 1) is always higher or  
 421 equal to the value  $k = k^*$  predicted by EV and EE theories, 2) depends only on  $\alpha$  and 3) can  
 422 again be found from the scaling properties of the rainfall process. The excess of  $I_r$  above  
 423 thresholds on the order of the  $(cr^\alpha)$ -year maximum has  $GP(k_\alpha)$  distribution with the same value  
 424 of  $k_\alpha$ . The value  $k = k^*$  from classical EV and EE analysis is recovered for  $\alpha$  larger than a  
 425 critical value  $\alpha^*$ . Therefore, in the context of multifractal models, our analysis generalizes the  
 426 results of classical EV and EE theories. Note that using  $k^*$  instead of  $k_\alpha$  would result in  
 427 underestimation of the probability of extreme rainfalls.

428 At the root of the differences between our results and those of classical EV theory is that  
 429 the settings under which the results are obtained are different: In EV analysis one fixes the  
 430 resolution  $r$  and considers the distribution of the maximum of  $n$  independent copies of  $I_r$  as  
 431  $n \rightarrow \infty$ . The asymptotic EV results are commonly assumed to apply to the annual maxima, at  
 432 least at high resolutions  $r$ . By contrast, in the LD analysis one lets  $r \rightarrow \infty$  while setting  $n$  to the  
 433 number of resolution- $r$  intervals in one year. In the latter formulation,  $n$  varies with  $r$  in a way  
 434 that makes sense for the study of the annual maxima at small scales.

435 Other important results we have obtained concern the distribution of the annual maximum  
 436  $I_{yr, r}$  for finite  $r$ . In this case the distribution is not GEV, but over a range of quantiles of  
 437 practical interest can be accurately approximated by a  $GEV(k)$  distribution. We have found that  
 438 the best-fitting shape parameter  $k$  increases with increasing resolution  $r$ , in a way consistent with  
 439 findings from directly fitting GEV distributions to annual maximum data; see Section 4. The  
 440 best-fitting  $k$  generally remains within the EV2 range, but at large scales it is close to zero (EV1  
 441 fit). This finding is important, as it explains why an EV2 distribution often fits well the annual  
 442 maximum data and why the shape parameter depends on the resolution (in contrast with the

443 asymptotic EV prediction that  $k$  is constant with  $r$ ). The best-fitting  $k$  depends little on the range  
444 of quantiles used in the fit and is not very sensitive to the scaling parameters, within the range of  
445 values that are typical for rainfall (except that  $k$  tends to be somewhat higher in dry than in wet  
446 climates). Taking advantage of this lack of sensitivity, we have obtained default values of  $k$  as a  
447 function of  $r$ , which can be used at non-instrumented sites or in cases of very short rainfall  
448 records.

449       The above results are significant in several respects. The asymptotic findings (1) show that  
450 large-deviation theory should find a place in stochastic hydrology at least as prominent as EV  
451 and EE theories and (2) indicate that what matters for the annual maximum rainfall is usually not  
452 the upper tail of the parent distribution, but a range of that distribution closer to the body. In  
453 addition, the pre-asymptotic analysis (1) shows that GEV models accurately approximate the  
454 non-GEV distribution of the annual maximum, (2) indicates that the shape parameter  $k$  of the  
455 approximating GEV distribution varies with resolution  $r$ , and (3) produces new ways to estimate  
456  $k$ , from the scaling properties of rainfall.

457       This line of inquiry should continue. There is evidence that rainfall satisfies multifractal  
458 scale-invariance only in approximation, over a finite range of scales (typically between about 1  
459 hour and several days) and under certain conditions (for example only within rainstorms); see  
460 e.g. Schmitt *et al.*, (1998), Sivakumar *et al.* (2001), Veneziano *et al.* (2006b) and Veneziano and  
461 Langousis (2009). It would be interesting to examine the sensitivity of our results to the structure  
462 of the rainfall model. Specific alternatives to our multifractal representation are bounded  
463 cascades (see e.g Menabde *et al.*, 1997 and Menabde, 1998), which retain the multiplicative  
464 structure but allow the intensity of the fluctuations to vary with scale, and models that explicitly

465 recognize rainstorms and dry inter-storm periods and assume scale invariance (or bounded-  
 466 cascade behavior) within the storms (e.g. Langousis and Veneziano, 2007).

467 A notoriously difficult problem is to estimate the shape parameter  $k$  of the annual  
 468 maximum distribution from at-site information (see e.g. Koutsoyiannis, 2004). This is why one  
 469 often resorts to regionalization. The finding that  $k$  is determined not by the upper tail of  $I_r$  but by  
 470 regions of the distribution closer to the body and can be calculated from the scaling properties of  
 471 rainfall opens new possibilities for both at-site and regionalized estimation of this parameter.  
 472 Developments in this direction will be the subject of follow-up communications.

### 473 **Appendix A: Small-Scale Behavior of Certain Quantiles of $I_r$**

474 Let  $i$  be the value exceeded by  $I_r$  with probability  $\eta D / (cr^{1+\alpha})$ , where  $c$  and  $D$  are given positive  
 475 constants. We are interested in how, as the resolution  $r \rightarrow \infty$ ,  $i$  varies with  $r$  and  $0 < \eta < \infty$ , for  
 476 different  $\alpha$ . For this purpose, we write  $i$  as  $r^\gamma$  and use equation (7) to find  $\gamma$  such that  $P[I_r > r^\gamma]$   
 477  $= \eta D / (cr^{1+\alpha})$ .

478 Suppose first that  $\gamma \leq \gamma^*$ , where  $\gamma^*$  is the slope of  $K(q)$  at  $q^*$  (as we shall see,  $\gamma$  does not  
 479 exceed  $\gamma^*$  if  $\alpha$  does not exceed a related threshold  $\alpha^*$ ). Then equation (7) gives

$$480 \quad P[I_r > r^\gamma] \sim r^{-C(\gamma)} \quad (\text{A.1})$$

481 We want  $\gamma$  such that the right hand side of equation (A.1) equals  $\eta D / (cr^{1+\alpha})$ . Therefore  $\gamma$  must  
 482 satisfy

$$483 \quad C(\gamma) = (1 + \alpha) + \log_r \left( \frac{c}{\eta D} \right) \quad (\text{A.2})$$

484 For any finite  $c$ ,  $b$  and  $D$ ,  $\log_r[c/(\eta D)] \rightarrow 0$  as  $r \rightarrow \infty$ . Hence one may replace  $C(\gamma)$  in equation  
 485 (A.2) with its linear Taylor expansion around the value  $\gamma_{1+\alpha}$  such that  $C(\gamma_{1+\alpha})=1+\alpha$ . Using  
 486 equation (5), this gives

$$487 \quad C(\gamma) = (1 + \alpha) + q_{1+\alpha}(\gamma - \gamma_{1+\alpha}) \quad (\text{A.3})$$

488 where  $q_{1+\alpha}$  is the moment order at which the slope of  $K(q)$  in equation (4) equals  $\gamma_{1+\alpha}$  and is  
 489 also the derivative of  $C(\gamma)$  at  $\gamma_{1+\alpha}$ ; see Figure 1. Equating the right hand sides of equations  
 490 (A.2) and (A.3), one obtains

$$491 \quad \gamma = \gamma_{1+\alpha} + \frac{1}{q_{1+\alpha}} \log_r\left(\frac{c}{\eta D}\right) \quad (\text{A.4})$$

492 We conclude that, for large  $r$  and any given  $c$  and  $D$ ,  $i = r^\gamma$  satisfies

$$493 \quad i \sim r^{\gamma_{1+\alpha}} \eta^{-1/q_{1+\alpha}} \quad (\text{A.5})$$

494 Equation (A.5) holds for  $\gamma_{1+\alpha} \leq \gamma^*$ , or equivalently for  $\alpha \leq \alpha^*$ , where  
 495  $\alpha^* = C(\gamma^*) - 1 = q^*(\gamma^* - 1)$ .

496 For  $\alpha > \alpha^*$ ,  $\gamma$  exceeds  $\gamma^*$  and one must use the second expression in equation (7).

497 Therefore  $\gamma$  must satisfy

$$498 \quad C(\gamma^*) + q^*(\gamma - \gamma^*) = (1 + \alpha) + \log_r\left(\frac{c}{\eta D}\right) \quad (\text{A.6})$$

499 Solving for  $\gamma$  and using  $C(\gamma^*) = 1 + \alpha^*$  gives the following expression for  $i = r^\gamma$ :

$$500 \quad i \sim r^{\gamma^* + (\alpha - \alpha^*)/q^*} \eta^{-1/q^*} \quad (\text{A.7})$$

501 The results in equations (A.5) and (A.7) are reproduced in equation (9).

502  
503  
504  
505  
506  
507  
508  
  
509  
510  
511  
512  
513  
514  
515  
516  
517  
518  
519  
520  
521  
522  
523  
524  
525  
526  
527

### Acknowledgments

This work was supported by project RISK (High Speed Rail) of the M.I.T.-Portugal Program (MPP), project POCI/GEO/59712/2004 of the Portuguese Foundation for Science and Technology (FCT), and the NSF Award # EAR-0910721. The second author was also partially supported by the Alexander S. Onassis Public Benefit Foundation under Scholarship No. F-ZA 054/2005-2006. We thank Bellie Sivakumar and two anonymous reviewers for their comments and suggestions.

### References

Asquith, W.H. (1998) Depth-Duration Frequency of Precipitation for Texas, Water-Resources Investigations Report 98-4044, U.S. Geological Survey, <http://pubs.usgs.gov/wri/wri98-4044/pdf/98-4044.pdf>.

Beirlant, J., J.L. Teugels and P. Vynckier (1996) *Practical Analysis of Extreme Values*, Leuven University Press Blijde-Inkomststraat 5, B-3000 Leuven (Belgium), pp. 137.

Caporali, E., E. Cavigli and A. Petrucci (2006) Regional Frequency Analysis of Rainfall extremes in Tuscany (Italy), International Workshop on Hydrological Extremes “Observing and Modelling Exceptional Floods and Rainfalls”, Rende (CS), 3-4 May 2006.

Chow, V.T., D.R. Maidment and L.W. Mays (1988) *Applied Hydrology*, McGraw-Hill, New York.

Cramer, H. (1938) Sur un Nouveau Theoreme-limite de la Theorie des Probabilites, *Actualites Scientifiques et Industrielles*, No. 736 of Colloque consacre a la theorie des probabilités, Herrman, Paris, pp. 5-23.

Deidda, R. (2000) Rainfall Downscaling in a Space-time Multifractal Framework, *Wat. Resour. Res.*, **36**(7), 1779-1794.

Dembo, A. and O. Zeitouni O (1993) *Large Deviation Techniques and Applications*, Jones and Barlett, Boston.

- 528 Den Hollander, F. (2000) *Large Deviations*, American Mathematical Society.
- 529 Evertsz, C.J.G. and B.B. Mandelbrot (1992) Appendix B of *Chaos and Fractals*, eds. H.-O.  
530 Peitgen, H. Jurgens, and D. Saupe, Springer-Verlag.
- 531 Gellens, D. (2002) Combining Regional Approach and Data Extension Procedure for Assessing  
532 GEV Distribution of Extreme precipitation in Belgium, *J. Hydrol.*, **268**, 113-126.
- 533 Güntner, A., J. Olsson, A. Calver and B. Gannon (2001) Cascade-based Disaggregation of  
534 Continuous Rainfall Time Series: The Influence of Climate, *Hydrol. Earth Syst. Sci.*, **5**,  
535 145-164.
- 536 Gumbel, E.J. (1958) *Statistics of Extremes*, Columbia University Press, New York.
- 537 Gupta, V. K. and E. Waymire (1990) Multiscaling Properties of Spatial Rainfall and River Flow  
538 Distributions, *J. Geophys. Res.*, **95** (D3), 1999-2009.
- 539 Hosking, J.R.M. (1990) L-moments: Analysis and Estimation of Distributions Using Linear  
540 Combinations of Order Statistics. *J. Roy. Statist. Soc. Ser. B*, **52**, 105–124.
- 541 Hosking, J.R.M. (1992), Moment or L Moments? An Example Comparing two Measures of  
542 Distributional Shape, *The American Statistician*, **46**(3), 186-189.
- 543 Kahane, J.P. and J. Peyriere (1976) Sur certaines martingales de Benoit Mandelbrot, *Adv. Math.*,  
544 **22**: 131-145.
- 545 Koutsoyiannis, D. (2004) Statistics of Extremes and Estimation of Extreme Rainfall: II.  
546 Empirical Investigation of Long Rainfall Records, *Hydrolog. Sci. J.*, **49**(4), 591– 610.
- 547 Koutsoyiannis, D., D. Kozonis and A. Manetas (1998) A Mathematical Framework for Studying  
548 Rainfall Intensity-Duration-Frequency Relationships, *J. Hydrol.*, **206**, 118-135.
- 549 Langousis A, D. Veneziano, P. Furcolo, and C. Lepore (2007) Multifractal Rainfall Extremes:  
550 Theoretical Analysis and Practical Estimation, *Chaos Solitons and Fractals*,  
551 doi:10.1016/j.chaos.2007.06.004.
- 552 Langousis, A. and D. Veneziano (2007) Intensity-duration-frequency curves from Scaling  
553 Representations of Rainfall, *Wat. Resour. Res.*, **43**, doi: 10.1029/2006WR005245.

- 554 Leadbetter, M.R. (1991) On a Basis for “Peak over Threshold” Modeling, *Statistics &*  
555 *Probability Letters*, **12**, 357-362.
- 556 Lepore, C., D. Veneziano and A. Langousis (2009) Annual Rainfall Maxima: Practical  
557 Estimation Based on Large-Deviation Results, European Geosciences Union, Vienna,  
558 Austria, April 2009.
- 559 Madsen, H., P.F. Rasmussen and D. Rosbjerg (1997) Comparison of Annual Maximum Series  
560 and Partial Duration Series Methods for Modeling Extreme Hydrologic Events 1. At-site  
561 Modeling, *Wat. Resour. Res.*, **33**(4), 747-757.
- 562 Martins, E.S. and J.R. Stedinger (2001a) Historical Information in a Generalized Maximum  
563 Likelihood Framework With Partial Duration and Annual Maximum Series, *Water*  
564 *Resour. Res.*, **37**(10), 2559–2567.
- 565 Martins, E.S. and J.R. Stedinger (2001b) Generalized Maximum Likelihood Pareto-Poisson  
566 Estimators For Partial Duration Series, *Water Resour. Res.*, 37(10), 2551–2557.
- 567 Martins, E.S. and J.R. Stedinger (2000) Generalized Maximum-likelihood Generalized Extreme-  
568 value Quantile Estimators for Hydrologic Data, *Wat. Resour. Res.*, **36**(3), 737-744.
- 569 Menabde, M. (1998) Bounded Lognormal Cascades as Quasi-Multiaffine Random Fields,  
570 *Nonlinear Processes Geophys.* **5**, 63-68.
- 571 Menabde, M., D. Harris, A. Seed, G. Austin and D. Stow (1997) Multiscaling Properties of  
572 Rainfall and Bounded Random Cascades, *Wat. Resour. Res.*, **33**(12), 2823-2830.
- 573 Mohyont, B., G.R. Demareé, D.N. Faka (2004) Establishment of IDF-curves for Precipitation  
574 in the Tropical Area of Central Africa: Comparison of Techniques and Results, *Nat. Haz.*  
575 *Ear. Sys. Sci.*, **4**, 375-387.
- 576 Olsson, J. (1998) Evaluation of a Scaling Cascade Model for Temporal Rain-fall Disaggregation,  
577 *Hydrol. Earth Syst. Sci.*, **2**, 19-30.
- 578 Over, T.M. and V.K. Gupta (1996) A Space-Time Theory of Mesoscale Rainfal Using Random  
579 Cascades, *J. Geophys. Res.*, **101**(D21), 26 319- 26 331.
- 580 Overeem, A., A. Buishand, and I. Holleman (2008) Rainfall Depth-duration-frequency Curves  
581 and their Uncertainties, *J. Hydrol.*, **348**, 124-134.

- 582 Perica, S. and E. Foufoula-Georgiou (1996) Model for Multiscale Disaggregation of Spatial  
583 Rainfall Based on Coupling Meteorological and Scaling Descriptions. *J. Geophys. Res.*,  
584 **101**(D21), 26347-26361.
- 585 Pickands, J. (1975) Statistical inference using extreme order statistics, *Ann. Statist.* **3**, 119-131.
- 586 Schertzer, D. and S. Lovejoy (1987) Physical Modeling and Analysis of Rain and Clouds by  
587 Anisotropic Scaling of Multiplicative Processes, *J. Geophys. Res.*, **92**, 9693-9714.
- 588 Schmitt, F., S. Vannitsem, and A. Barbosa (1998) Modeling of Rainfall Time Series Using Two-  
589 state Renewal Processes and Multifractals, *J. Geophys. Res.*, **103**(D18)**92**, 23181-23193.
- 590 Singh, V.P. (1992) *Elementary Hydrology*, Prentice-Hall, New Jersey, U.S.A.
- 591 Sivakumar, B., S. Sorooshian, H.V. Gupta and X. Gao (2001). A Chaotic Approach to Rainfall  
592 Disaggregation, *Wat. Resour. Res.*, **37**(1), 61-72.
- 593 Smith, R.L. (1985) Threshold Methods for Sample Extremes, in J. Tiago de Oliveira, ed.,  
594 *Statistical Extremes and Applications*, NATO ASI Series (Reidl, Dordrecht), pp. 623-  
595 638.
- 596 Stedinger, J.R., R.M. Vogel and E. Foufoula-Georgiou (1993) Frequency Analysis in Extreme  
597 Events, in *Handbook of Applied Hydrology*, edited by D. A. Maidment, Ch. 18, pp. 18.1-  
598 18.66, McGraw-Hill, New York.
- 599 Trefry, C.M., D.W. Watkins Jr. and D. Johnson (2005) Regional Rainfall Frequency Analyses  
600 for the State of Michigan, *J. Hydrol. Eng.*, **10**(6): 437-449.
- 601 Vaskova, I. (2005) Rainfall Analysis and Regionalization Computing Intensity-Duration-  
602 Frequency Curves, [www.lyon.cemagref.fr/projets/floodaware/report/05upv1.pdf](http://www.lyon.cemagref.fr/projets/floodaware/report/05upv1.pdf)
- 603 Veneziano D. and A. Langousis (2009) Scaling and Fractals in Hydrology, In: *Advances in Data-*  
604 *based Approaches for Hydrologic Modeling and Forecasting*, Edited by: B. Sivakumar,  
605 World Scientific (in press).
- 606 Veneziano, D. (1999) Basic Properties and Characterization of Stochastically Self-similar  
607 Processes in  $R^d$  *Fractals*, **7**, 59.
- 608 Veneziano, D. (2002) Large Deviations of Multifractal Measures, *Fractals*, **10**, 117-129.  
609 Erratum in *Fractals*, 2005; **13**(2), 1-3.

- 610 Veneziano, D. and A. Langousis (2005a) The Areal Reduction Factor a Multifractal Analysis,  
611 *Wat. Resour. Res.*, **41**, W07008, doi:10.1029/2004WR003765.
- 612 Veneziano, D. and A. Langousis (2005b) The Maximum of Multifractal Cascades: Exact  
613 Distribution and Approximations, *Fractals*, **13**(4), 311-324.
- 614 Veneziano, D., A. Langousis and P. Furcolo (2006a) Multifractality and Rainfall Extremes: A  
615 Review, *Wat. Resour. Res.*, **42**, W06D15, doi:10.1029/2005WR004716.
- 616 Veneziano, D., C. Lepore, A. Langousis and P. Furcolo (2007) Marginal Methods of IDF  
617 Estimation in Scaling and Non-Scaling Rainfall, *Water Resour. Res.*, **43**, W10418,  
618 doi:10.1029/2007WR006040.
- 619 Veneziano, D., P. Furcolo and V. Iacobellis (2006b) Imperfect Scaling of Time and Space-Time  
620 Rainfall, *J. Hydrol.*, **322**(1-4), 105-119.
- 621 Veneziano, D., R.L. Bras and J.D. Niemann (1996) Nonlinearity and Self-similarity of Rainfall  
622 in Time and a Stochastic model, *J. Geophys. Res.*, **101**(D21), 26371- 26392.
- 623 Venugopal, V., E. Foufoula-Georgiou and V. Sapozhnikov (1999) Evidence of Dynamic  
624 Scaling in Space Time Rainfall, *J. Geophys. Res.*, **104**(D24), 31599-31610.

## Figure Captions

625

626 Figure 1: Illustration of the moment scaling function  $K(q)$  and its Legendre transform  $C(\gamma)$  in  
627 equation (6).

628 Figure 2: Shape parameter  $k_\alpha$  of the  $N$ -year maximum of  $I_r$  under ( $r \rightarrow \infty$ ,  $N = cr^\alpha$ ). Beta-  
629 lognormal rainfall process with  $C_\beta = 0.4$  and  $C_{LN} = 0.05$ . Larger values of  $k$   
630 correspond to higher probabilities of exceedance of extreme rainfalls.

631 Figure 3: Schematic illustration of asymptotic results on rainfall maxima from extreme value  
632 (EV) and large deviation (LD) theories.

633 Figure 4: GEV( $k$ ) approximations to the exact distribution of the annual maximum  $I_{yr,r}$  at  
634 resolutions  $r = 1$  and 512, in the return-period range from 2-10 000 years. The top row  
635 shows the best least-squares fit on GEV( $k$ ) paper and gives the associated value of  $k$ .  
636 The lower rows show plots on GEV( $k$ ) paper for  $k = 0$  (EV1 paper),  $k^* = 1/q^*$  (value  
637 predicted by EV and EE theories), and  $k_0 = 1/q_1$  (value predicted by LD theory for  
638  $r \rightarrow \infty$ ). Deviations of the plots from a straight line indicate lack of fit for the selected  
639 value of  $k$ .

640 Figure 5: Dependence of the least-squares shape parameter  $k$  on the resolution  $r = D/d$ . (a)  
641 Theoretical values of  $k$  for  $C_\beta = 0.4$  and  $C_{LN} = 0.05$  when fitting is over the return  
642 period range from 2-100 years. The vertical bars are  $(m \pm \sigma)$  intervals for the  
643 probability weighted moments (PWM) estimator of  $k$  using the annual maxima from  
644 100-year continuous multifractal process simulations. The values  $k^* = 1/q^*$  and  
645  $k_0 = 1/q_1$  are shown for reference. (b) Comparison of the theoretical values of  $k$  from  
646 (a) with empirical estimates from the literature assuming an average value of  $D = 15$   
647 days.

648 Figure 6. (a) Best-fitting shape parameters  $k$  at different resolutions  $r$  for selected combinations  
649 of  $C_\beta$  and  $C_{LN}$ . The range of return periods  $T$  used for fitting is from 2 - 100 years.  
650 (b) Estimates of  $C_\beta$  and  $C_{LN}$  from different rainfall records plotted against the mean  
651 annual precipitation. (c) Suggested default values of  $k$  as a function of the resolution  $r$   
652  $= D/d$ .

653  
654  
655  
656  
657  
658  
659  
660  
661  
662  
663  
664  
665  
666  
667  
668  
669  
670  
671  
672  
673  
674  
675  
676  
677  
678  
679  
680  
681  
682  
683  
684  
685  
686  
687  
688  
689  
690  
691

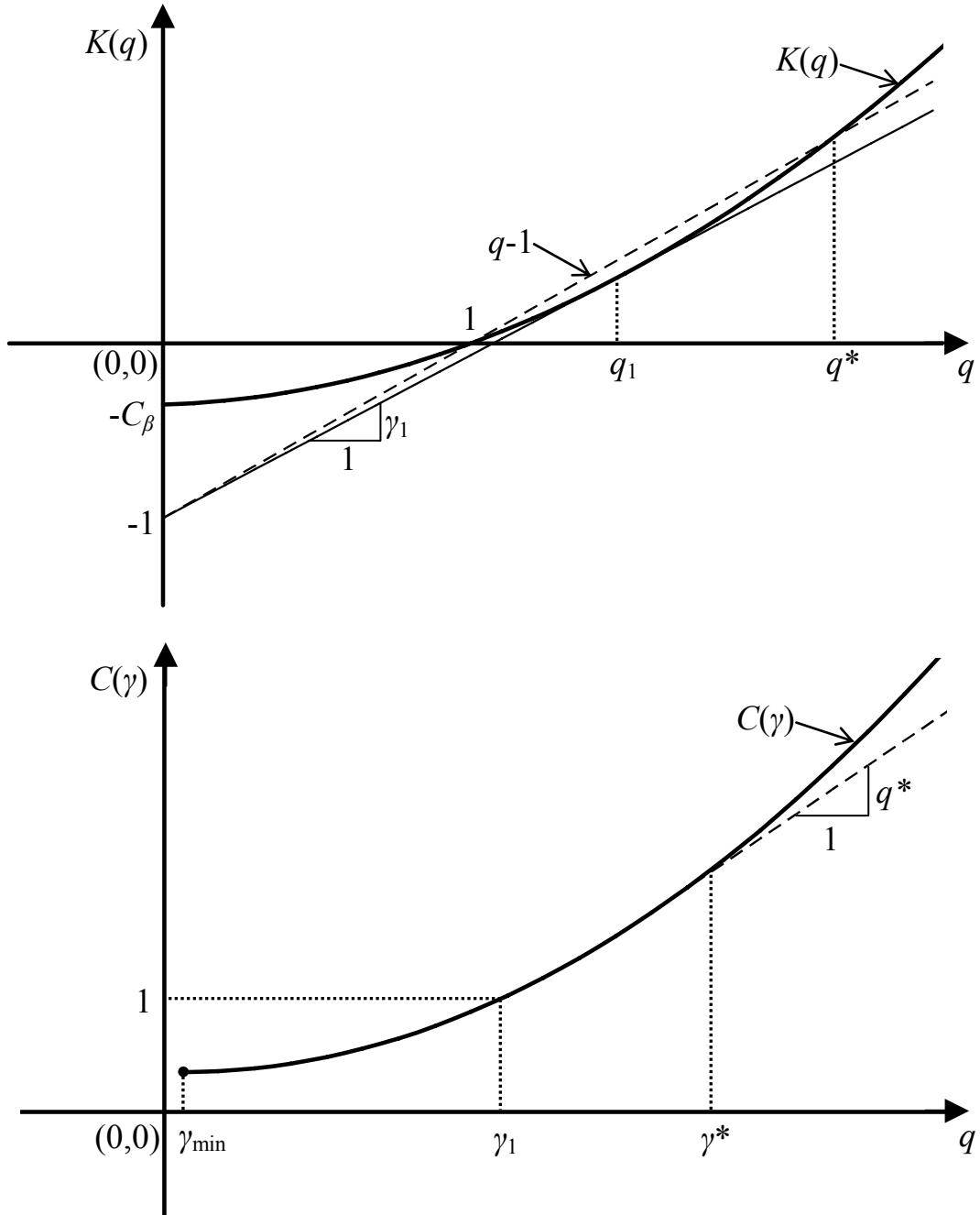


Figure 1: Illustration of the moment scaling function  $K(q)$  and its Legendre transform  $C(\gamma)$  in equation (6).

692  
 693  
 694  
 695  
 696  
 697  
 698  
 699  
 700  
 701  
 702  
 703  
 704  
 705  
 706  
 707  
 708  
 709  
 710  
 711  
 712  
 713  
 714  
 715  
 716  
 717  
 718  
 719  
 720

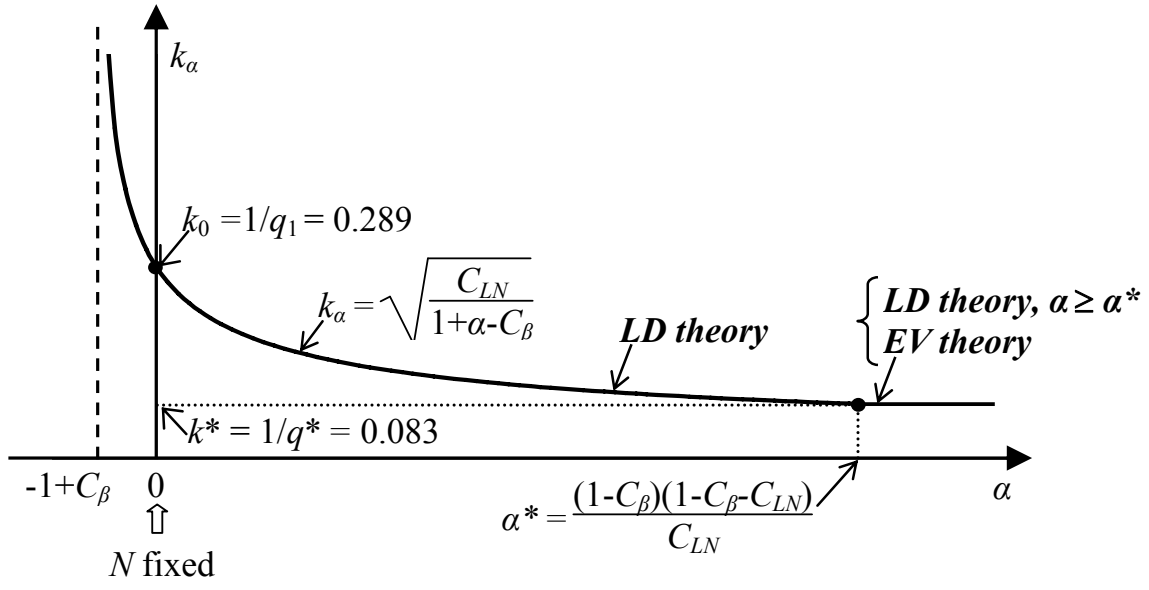
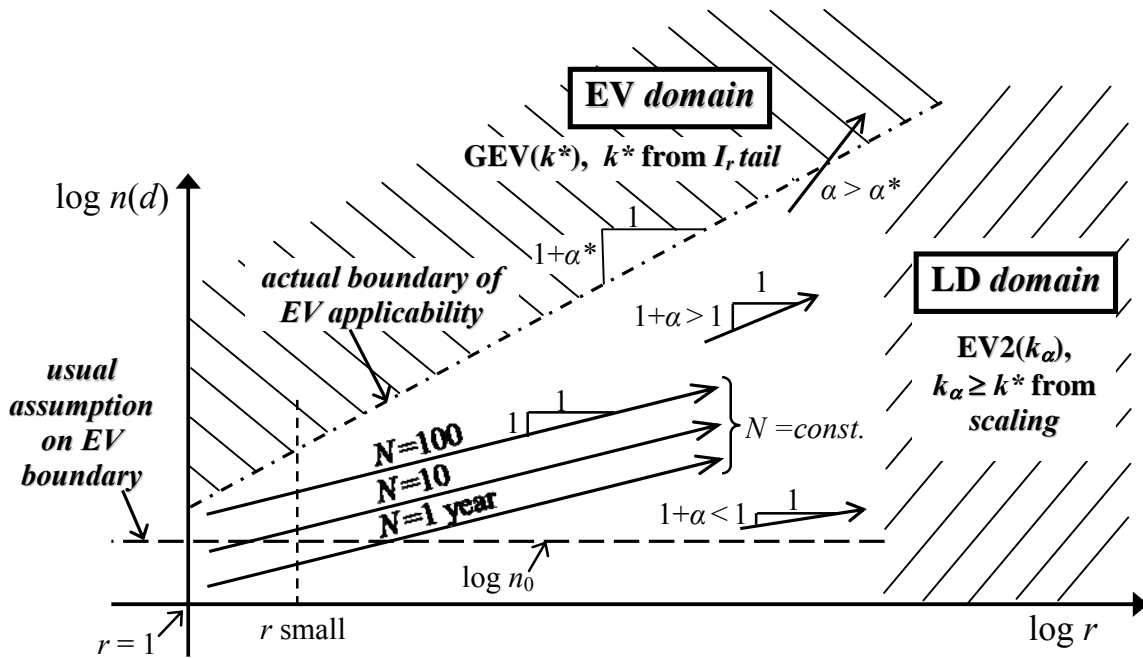
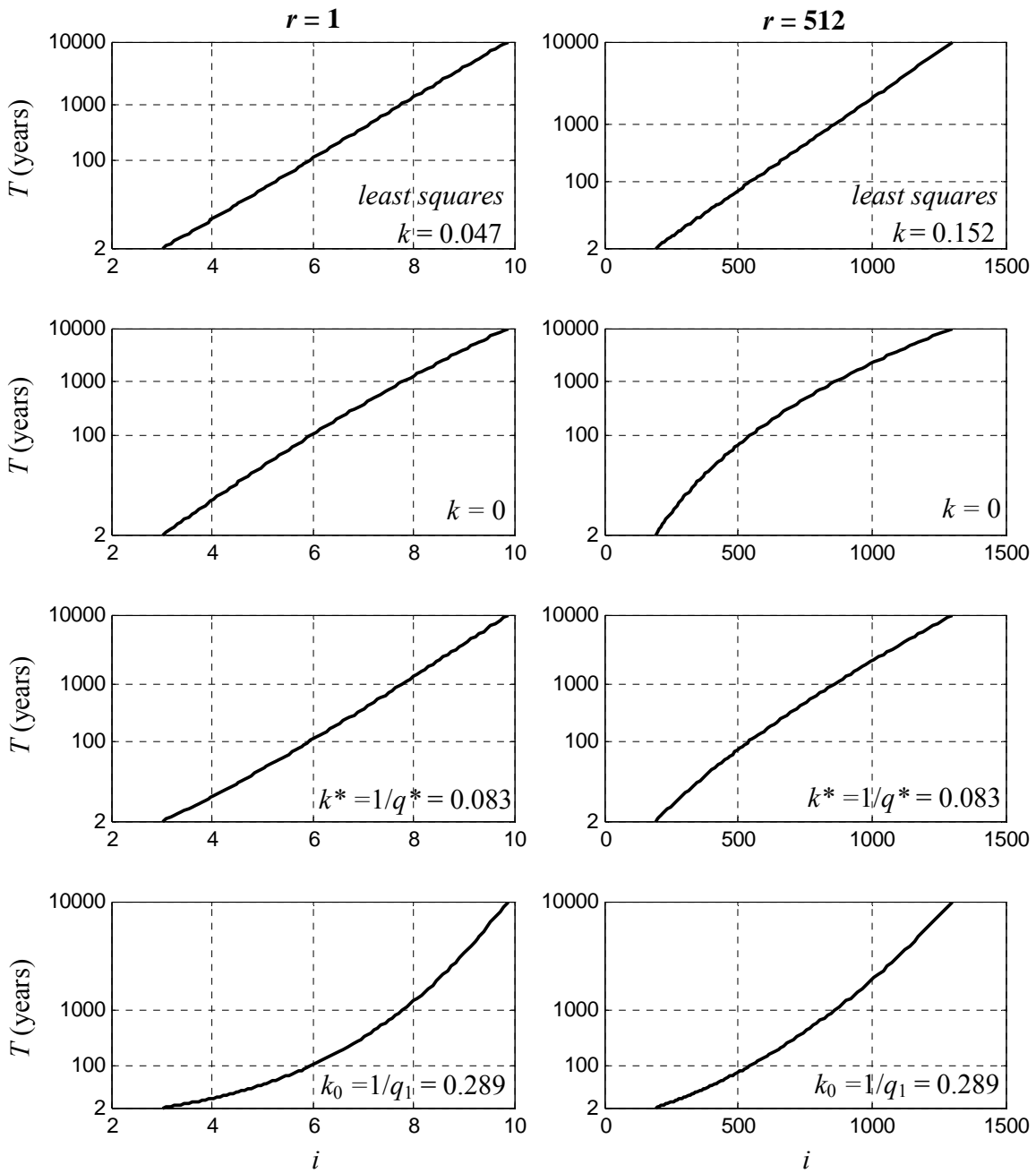


Figure 2: Shape parameter  $k_\alpha$  of the  $N$ -year maximum of  $I_r$  under  $(r \rightarrow \infty, N = cr^\alpha)$ . Beta-lognormal rainfall process with  $C_\beta = 0.4$  and  $C_{LN} = 0.05$ . Larger values of  $k$  correspond to higher probabilities of exceedance of extreme rainfalls.

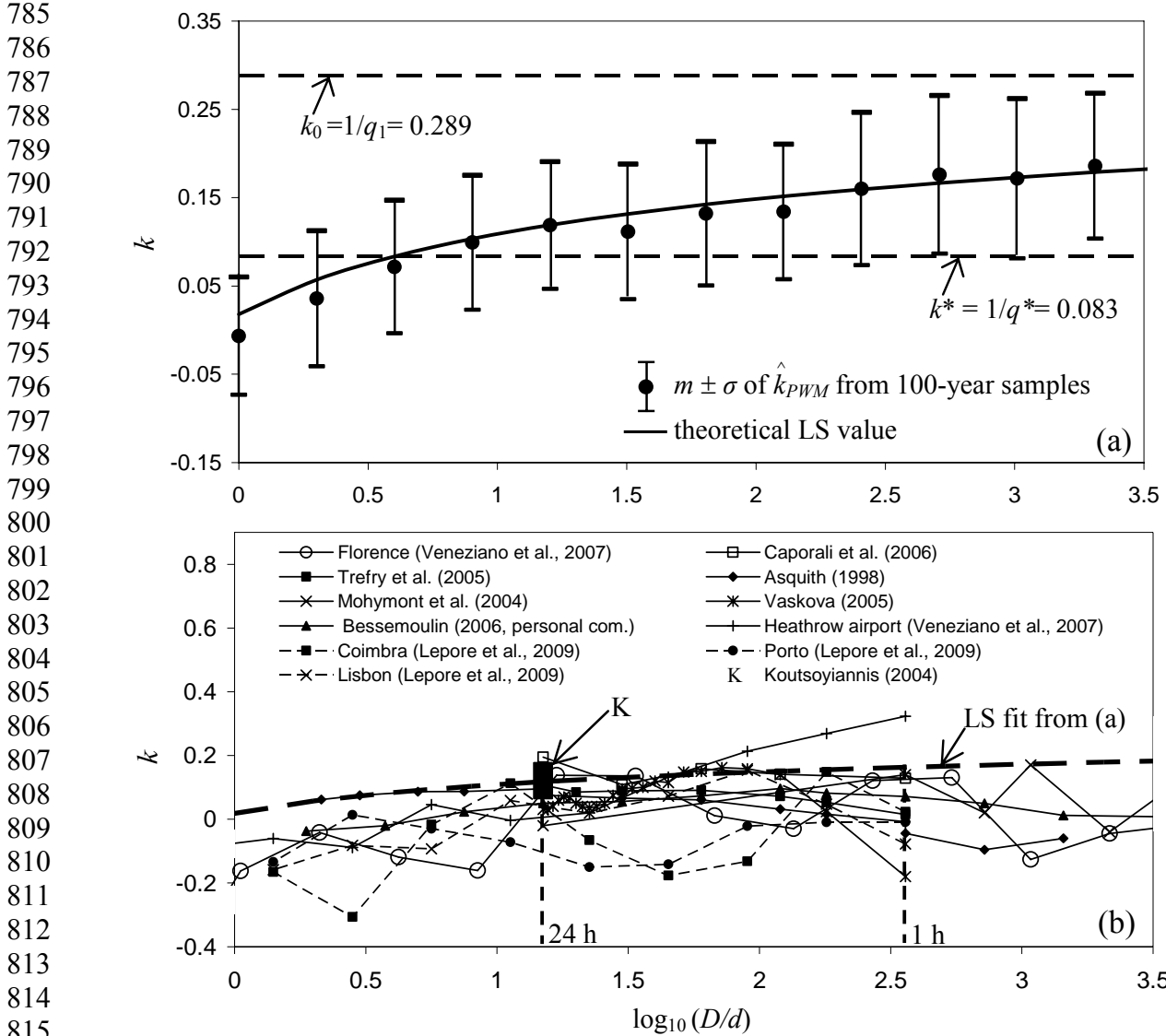


740 Figure 3: Schematic illustration of asymptotic results on rainfall maxima from extreme value  
 741 (EV) and large deviation (LD) theories.

742  
 743  
 744  
 745  
 746  
 747  
 748  
 749  
 750  
 751  
 752  
 753  
 754  
 755  
 756  
 757  
 758  
 759  
 760  
 761  
 762  
 763  
 764  
 765  
 766  
 767  
 768  
 769  
 770  
 771  
 772  
 773  
 774  
 775  
 776  
 777  
 778



779 Figure 4: GEV( $k$ ) approximations to the exact distribution of the annual maximum  $I_{yr,r}$  at  
 780 resolutions  $r = 1$  and 512, in the return-period range from 2-10 000 years. The top row shows the  
 781 best least-squares fit on GEV( $k$ ) paper and gives the associated value of  $k$ . The lower rows show  
 782 plots on GEV( $k$ ) paper for  $k = 0$  (EV1 paper),  $k^* = 1/q^*$  (value predicted by EV and EE theories),  
 783 and  $k_0 = 1/q_1$  (value predicted by LD theory for  $r \rightarrow \infty$ ). Deviations of the plots from a straight  
 784 line indicate lack of fit for the selected value of  $k$ .



816 Figure 5: Dependence of the least-squares shape parameter  $k$  on the resolution  $r = D/d$ . (a)  
817 Theoretical values of  $k$  for  $C_\beta = 0.4$  and  $C_{LN} = 0.05$  when fitting is over the return period range  
818 from 2-100 years. The vertical bars are  $(m \pm \sigma)$  intervals for the probability weighted moments  
819 (PWM) estimator of  $k$  using the annual maxima from 100-year continuous multifractal process  
820 simulations. The values  $k^* = 1/q^*$  and  $k_0 = 1/q_1$  are shown for reference. (b) Comparison of the  
821 theoretical values of  $k$  from (a) with empirical estimates from the literature assuming an average  
822 value of  $D = 15$  days.

823  
824  
825  
826  
827  
828  
829  
830  
831  
832  
833  
834  
835  
836  
837  
838  
839  
840  
841  
842  
843  
844  
845  
846  
847  
848  
849  
850  
851  
852  
853  
854  
855  
856  
857  
858  
859  
860  
861  
862  
863  
864  
865  
866  
867

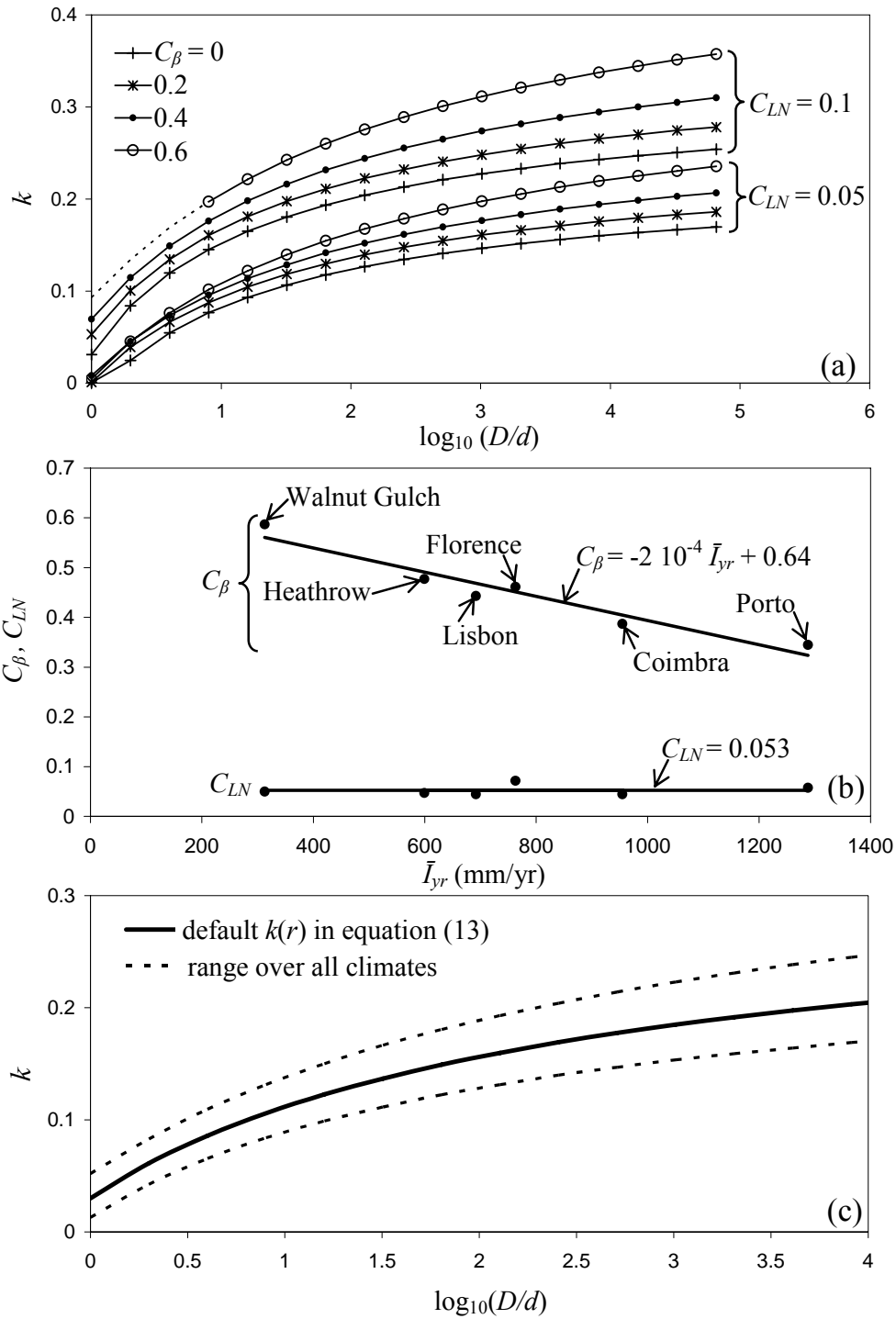


Figure 6. (a) Best-fitting shape parameters  $k$  at different resolutions  $r$  for selected combinations of  $C_\beta$  and  $C_{LN}$ . The range of return periods  $T$  used for fitting is from 2 - 100 years. (b) Estimates of  $C_\beta$  and  $C_{LN}$  from different rainfall records plotted against the mean annual precipitation. (c) Suggested default values of  $k$  as a function of the resolution  $r = D/d$ .